The earliest evidence for mechanically delivered projectile weapons in Europe

The earliest evidence for mechanically delivered projectile weapons in Europe

Katsuhiro Sano [1*], Simona Arrighi[2,3], Chiaramaria Stani[4], Daniele Aureli[3,5], Francesco Boschin[3], Ivana Fiore[6], Vincenzo Spagnolo[3], Stefano Ricci[3], Jacopo Crezzini[3], Paolo Boscato[3], Monica Gala[6], Antonio Tagliacozzo[6], Giovanni Birarda[4], Lisa Vaccari[4], Annamaria Ronchitelli[3], Adriana Moroni[3] and Stefano Benazzi[2,7]

[1]Center for Northeast Asian Studies, Tohoku University, Sendai, Japan. [2]Department of Cultural Heritage, University of Bologna, Ravenna, Italy. [3]Dipartimento di Scienze Fisiche, della Terra e dell'Ambiente, UR Preistoria e Antropologia, Università degli Studi di Siena, Siena, Italy. [4]Elettra-Sincrotrone Trieste S.C.p.A., Trieste, Italy. [5]UMR 7041, Équipe AnTET, Université de Paris X-Nanterre, Paris, France. [6]Bioarchaeological Service, Museo delle Civiltà, Museo Preistorico Etnografico "Luigi Pigorini", Rome, Italy. [7]Department of Human Evolution, Max Planck Institute for Evolutionary Anthropology, Leipzig, Germany. [*]e-mail: sano.k@tohoku.ac.jp

Microscopic analysis of backed lithic pieces from the Uluzzian technocomplex (45–40 thousand yr ago) at Grotta del Cavallo (southern Italy) reveals their use as mechanically delivered projectile weapons, attributed to anatomically modern humans. Use-wear and residue analyses indicate that the lithics were hunting armatures hafted with complex adhesives, while experimental and ethnographic comparisons support their use as projectiles. The use of projectiles conferred ahunting strategy with a higher impact energy and a potential subsistence advantage over other populations and species.

The Uluzzian was traditionally recognized as one of the Middle to Upper Palaeolithic transitional cultures in southern Europe (that is, Italy and Greece), but has been recently redefined as an Early Upper Palaeolithic culture1. Grotta del Cavallo (Fig. 1), excavated by A. Palma di Cesnola and P. Gambassini between 1963 and 1986, is a pivotal site for the Uluzzian because its stratigraphic sequence includes three main Uluzzian layers, EIII (archaic Uluzzian), EII-I (evolved Uluzzian) and D (final Uluzzian)[1] (Supplementary Fig. 1), sandwiched by the tephra Y-6 at 45.5 ± 1.0 thousand years ago (ka)[2] and Y-5 (Campanian Ignimbrite) at 39.85 ± 0.14 ka (refs.[2,3]). The Uluzzian technocomplex exhibits features that are typically associated with modern human assemblages (Supplementary Information 2) and characterized by the presence of ornaments, bone implements[4], colouring substances[5] and crescent-shaped backed pieces made on small blades or bladelets[1]. These crescent shaped backed pieces (also referred to as lunates or segments) are a hallmark[1,6] of the Uluzzian and exhibit no techno-morphological link to the Mousterian or Initial Upper Palaeolithic assemblages in Europe before the Uluzzian. Similar backed pieces on bladelets have been observed in East Africa, although there is no archaeological evidence indicating a route from East Africa into Europe[5]. To better understand the differences between the Uluzzian and earlier lithic traditions, as well as the importance of the emergence of this new technocomplex in Europe, it is crucial to identify the function of the backed pieces.

The excavations of Grotta del Cavallo unearthed numerous backed pieces[6], and we undertook a systematic use-wear analysis of a total of 146 of them from the three Uluzzian layers. This analysis indicates that the major function of the Uluzzian backed pieces was hunting (Supplementary Table

1). Only seven pieces were used for functions other than hunting (cutting and scraping). Out of the 146 backed pieces, 26 show 55 diagnostic impact fractures (DIFs), which form only when stone tips hit an animal target (Fig. 2). Among them, 9 backed pieces (34.6%) bear DIFs only at a single location, while 17 (65.4%) yield multiple DIF types (Supplementary Table 2 and Supplementary Fig. 2). As several projectile trials resulted in no fractures or only non-diagnostic ones[7,8], the number of DIFs indicates the minimum number of specimens used as hunting weapons. Six pieces showed microscopic linear impact traces (MLITs) as well (Fig. 2a,f), proving that they were securely used as hunting armatures. Most of the Uluzzian backed pieces showed residues on the back, suggesting that this portion was covered by a type of adhesive (Supplementary Fig. 3). We therefore performed Fourier transform infrared (FTIR) spectromicroscopy on these pieces to characterize the chemical nature of the residues and identified them as a mixture of both organic and inorganic components, mainly ochre, a plant/tree gum and beeswax. The main absorption bands attributed to the organic fraction are highlighted by the grey shaded areas in Fig. 2o (see Methods for more details). In addition, FTIR spectroscopy analyses of several red deposit and soil samples recovered from Grotta del Cavallo enabled us to rule out the presence of organic contaminants from the burial environment and to confirm the presence of ochre as a mixture of silicate and iron oxides by correlative scanning electron microscopy/energy dispersive X-ray (SEM/EDX) measurements (see Supplementary Figs. 4 and 5). Together, the results allowed us to postulate that the three adhesive components had been intentionally mixed, as known in the middle Upper Palaeolithic context[9].To reconstruct the hafting modes of Uluzzian backed pieces, the frequency of the DIF types (Supplementary Fig. 2) was compared with those obtained by projectile experiments with backed piece replicas[10,11]. The projectile experiments indicated that hafting as barbs resulted less often in multiple DIFs, compared with when the pieces were hafted as tips. Among the multiple DIF types, the type a2m (flute-like, burin-like or transverse fractures from bidirectional
ends) was dominant in the Cavallo backed pieces (Fig. 2b–f) and occurred only in experiments with tip hafting (straight/obliquehafting). We do not rule out the possibility that some Uluzzian backed pieces were hafted as barbs because of the relatively high frequency of type a2 (burin-like fracture from steep angle) (Fig. 2a), which occurred in barb hafting as well. However, the frequency of the DIF types suggests that several Uluzzian backed pieces were attached on the tip of a wooden shaft. Uluzzian backed pieces are notably small: complete or almost complete backed pieces with DIFs measured an average of 27.1 mm in length, 10.5 mm in width and 4.6 mm in thickness (Supplementary Fig. 6a). The tip cross-sectional area (TCSA) and tip cross-sectional perimeter (TCSP) of Cavallo backed pieces with DIFs were compared with those of ethnographic North American dart tips and arrowheads[12,13]. The box plots of the TCSA and TCSP of the Uluzzian backed pieces with DIFs fell within the range of those of North American ethnographic arrowheads, but were concentrated on a smaller range (Supplementary Fig. 6b,c). The Uluzzian backed pieces are significantly smaller than the ethnographic dart tips in terms of TCSA and TCSP (TCSA: $t = -9.414$, $P < 0.05$; TCSP: $t = -13.650$, $P < 0.05$), and even smaller than the ethnographic arrowheads (TCSA: $t = -2.773$, $P < 0.05$; TCSP: $t = -5.709$, $P < 0.05$). The extremely small dimensions of the Uluzzian backed pieces suggest that they are suitable for neither thrusting nor throwing spear tips (Supplementary Fig. 7a,b). Despite the small size, the DIFs found on Cavallo backed pieces are relatively large: the largest DIF measures 24.7 mm in length, and 9 DIFs are larger than 10 mm. Several pieces show a significant eduction in the body due to impact damage (Fig. 2b,d,e). Even if specimens retain almost their original length, they often bear elongated DIFs along the side or on

the surface. The lengths of several elongated DIFs (flute- and burin-like fractures) exceed 20% of theentire length of the backed pieces, and four DIFs have a length greater than half the entire length of the specimens (Supplementary Table 3). The relatively large dimensions of DIFs suggest that thebacked pieces were delivered at high impact velocities. As several Uluzzian backed pieces were hafted on the tip of a wooden shaft, the small dimensions of the backed pieces must reflect the small diameter of the shaft. If a thinner shaft is used, the total size of the hunting weapon is smaller. Therefore, large DIFs, as well as multiple DIF types, occur only when the impact velocity is as high as is found for mechanical delivery, such as by a spearthrower or bow[8]. Although the TCSA and TCSP values indicate that the projectile capability of the Uluzzian backed pieces is closer to that of the North American arrowheads than to that of dart tips, we do not have sufficient information to discriminate between them. Nonetheless, because of the assumed velocity based on the DIF pattern, it is more plausible that the Uluzzian backed pieces were projected
using either a spearthrower or a bow. A higher impact energy, however, requires more stable hafting, since otherwise, stone tips can easily be displaced. A complex mixture, characterized by the addition of beeswax and ochre, increases the mechanical properties of the adhesive, making it less brittle14. The use of the complex adhesive demonstrated by FTIR spectroscopy in this study suggests that hunters at Grotta del Cavallo used advanced hafting technology for projectiles with a higher impact velocity. While the mechanical projectile system enables a higher impact velocity and long-range shooting, fletching to the base of the shaft is necessary to propel armatures in a straight trajectory. The discovery of cut marks due to the removal of feathers from bird remainsat the Uluzzian site of Castelcivita (southern Italy) (Supplementary Information 3) indicates that the fletching technology was also practiced by the Uluzzian people. The multiple findings, such as use-wear patterns, significant smallness of the Uluzzian backed pieces and complex adhesives, for Grotta del Cavallo samples dated between 45 ka and 40 ka constitute the earliest evidence for the use of mechanically delivered projectile weapons in Europe, which is more than 20,000 years earlier than previously thought. In Europe, the earliest direct evidence for spearthrowers was found from a Solutrean layer at Combe Saunière, France, dated between ~23 ka and ~20 ka (ref. [15]), and for bows and arrows preserved in peat bogs at an Ahrensburgian site of Stellmoor, Germany, at 12.9–11.7 ka (ref. [16]). Taking into account that most of the ethnographic spearthrowers are made of perishable materials, such as wood[17], it is no wonder that we have only much younger archaeological remains of spearthrowers and bows and arrows. Neanderthals used wooden spears[18] and might also have used stone-tipped ones[19]. Their possible stone spear tips, including Levallois and Mousterian points, are overall much larger than the Upper Palaeolithic points[20]. Although micropoints recovered from layer E (Neronian) of Grotte Madrin, France, that might be ~5,000 years older than the Uluzzian appearance in Europe are significantly small[21,22], a systematic use-wear analysis is required to detect their function. Based on the current state of studies on Neanderthal hunting[23], their spears were basically hand delivered (thrusting or throwing), but not mechanically projected. Conversely, evidence from Africa suggests that modern humans innovated mechanically delivered projectile weapons before they expanded out of Africa[20,24].
Although the association between the Uluzzian technocomplex and modern humans has been challenged[25], the information currently available from Grotta del Cavallo links the Uluzzian to modern humans. In particular, the two deciduous teeth retrieved from the Uluzzian layers of Grotta del Cavallo were attributed to modern humans[26], and their association with the Uluzzian materials has been recently confirmed by excavation field notes[1] (Supplementary Information 1) and the stratigraphic sequence[2]. If further studies confirm the attribution of the Uluzzian to modern humans,

we suggest that modern humans equipped themselves with new projectile technology when they migrated into Europe at around 45 ka. Zooarchaeological data on faunal remains from Grotta del Cavallo indicate more intensive exploitation of young horses at the Uluzzian levels than that seen at the late Mousterian (Supplementary Information 4). Considering the fact that young horses are protected by stallions[27], the intensive hunting of young horses may reflect skilled long-range hunting in the Uluzzian. As mechanically delivered armatures allow more accurate hunting[28] while keeping a greater distance from potentially dangerous prey than hand-delivered hunting (but see ref. [29]), this new projectile technology could have offered modern humans an advantage in subsistence strategies.

Methods

Functional analysis. A use-wear analysis was undertaken via a low-power approach[30–33] and a high-power approach[34–37]. Out of the 146 backed pieces, 34 pieces were recovered from layer EIII, 60 pieces from layer EII-I, 30 pieces from spit E-D and 22 pieces from layer D. Traces were observed using a Hirox KH7700 digital microscope at magnifications ranging from ×20 to ×50 for macrotraces and from ×140 to ×480 for microwear traces. DIFs were analysed using projectile experiments with backed pieces[7,8,38,39]. The DIFs observed on archaeological materials were recorded using the microscope mode of the Olympus TG-4 digital camera. Besides DIFs, 11 backed pieces exhibited possible impact fractures, but we cannot rule out the possibility that they formed accidentally due to knapping, retouching or post-depositional processes[7,39–41]. For instance, pseudo-impact fractures, including tiny flute- and burin-like fractures smaller than 5 mm, can occur throughout production and post-depositional processes. We therefore did not define these fractures as DIFs. The use of the bipolar technique on an anvil in retouching the Uluzzian backed pieces may create specific pseudo-impact fractures. We therefore conducted an experiment on the production of Uluzzian backed pieces to avoid the risk of misidentifying bipolar pseudo-impact scars as DIFs. After the careful observation of experimental backed pieces, we confirmed that although bipolar retouching sometimes produces mimic DIFs, we can distinguish these from real DIFs using the presence of a negative bulb of percussion and the position of the fracture initiation (Supplementary Fig. 8).MLITs are microscopically observable impact scars on lithic surfaces[7,8,42,43]. They comprise clusters of linear polishes running parallel to one another, exhibiting long shining stripes. Although little is known about the process of MLIT formation, they probably formed through contact with fragments detached from stone tips or the bones of animal targets. Similar linear polishes can occur through knapping by a hammer (Supplementary Fig. 8f) and contact with other stone artefacts during transport or storage[37]. However, it is possible to distinguish MLITs from the other linear polishes on the basis of attributes characterized by long, stripe-like linear polishes running in a specific direction with other linear polishes. The MLITs were recorded using a Hirox microscope at magnifications between ×140 and ×480.

Residue analysis. FTIR analyses were performed at the Chemical and Life Sciences branch of the SISSI beamline at Elettra Sincrotrone, Trieste[44]. Ten backed pieces were analysed by FTIR spectromicroscopy (100a from layer D; 106 from spit E-D; 75, 1, 34, 64, 45 and 52 from layer EII-I; and 21 and 23 from layer EIII). A few grains of the adherent residues were gently scraped from each backed piece using the tip of a needle under a stereomicroscope. Collected grains from each sample were pressed in a diamond compression cell (Diamond EX press by S.T. Japan, clear aperture 2 mm) to flatten them to a thickness suitable for FTIR transmission measurements. Owing to the heterogeneous nature of the samples, 10–15 spectra for each were acquired in transmission

mode on half compression cell with a Vis-IR Bruker Hyperion 3000 microscope coupled with the Vertex 70v interferometer in the MidIR range (MCT-A detector, 4,000–750 cm−1). For each spectrum, 512 scans were averaged at 4 cm−1 spectral resolution, setting the lateral resolution at 50 × 50 μm2 to select the most diagnostic sample regions according to the observable differences in colour. Spectra of red deposits from layers E and D and soil samples from several stratigraphic units belonging to Grotta del Cavallo (see Supplementary Fig. 1) were also measured by FTIR spectroscopy in the sample compartment of the Vertex 70v interferometer, in the closed diamond compression cell, using a 5 multiplication focusing unit (A524/Q, Bruker Optics) and the Bruker wide range components (that is, beamsplitter and DTGS detector) for covering FIR (far-infrared) and MIR (mid-infrared) spectral regions in a single scan. Each spectrum was collected averaging 256 scans at 4 cm−1. Extending the spectral range from 4,000 to 150 cm−1 allows better highlighting of the presence of metal-organic spectral features. To identify a specific material adhered on lithics, all of the acquired FTIR spectra were compared with those reported in the literature and IR spectral libraries (Kimmel Center for Archaeological Science Infrared Standards Library and IRUG Spectral Database). In addition, samples 1 and 106 were peeled off with carbon conductive adhesive tape from the culet of the diamond after FTIR spectromicroscopy analysis and SEM/EDX measurements were performed. Two red deposits (one from layer D and one from layer EII-I) and a sample of soil from layer DII were also characterized from a mineralogical perspective. All measurements were performed using a Zeiss Supra 40 field emission gun, an SEM equipped with a Gemini column and an in-lens secondary electron detector operated at 10 kV. EDX analyses were performed using a LN2-free X-Act Silicon Drift Detector (Oxford X-ray detection system, Aztec EDS). SEM/EDX measurements were performed at the IOM-CNR laboratories. Among the 10 backed pieces analysed by FTIR spectromicroscopy, only 6 (1, 34, 64, 106, 100a and 75) showed clear infrared features indicative of an organic fraction (see Fig. 2o). The organic fraction was verified by strong absorption peaks in the range 3,000–2,800 cm−1, which were assigned to methyl and methylene asymmetric and symmetric stretching modes at ~2,956 and ~2,872 cm−1, and ~2,930 and ~2,860 cm−1, respectively[45]. At ~1,460 and ~1,378 cm−1, the bending modes of the same moieties can be observed. The aforementioned stretching and bending modes are characteristic of compounds containing long aliphatic chains. In addition, carbonyl (C = O) bands can be detected at around 1,740 cm−1 for all the selected six samples, and an extra shoulder centred at about 1,715 cm−1 can be seen for samples 34, 64, 75 and 100a. Typically, carbonyl stretching modes of esters and carboxylic acids fall in this spectral region[46]. Samples 75, 106 and 100a (Fig. 2o) are characterized by two broad bands in the 1,650–1,550 cm−1 and 1,450–1,350 cm−1 spectral regions. The two aforementioned contributions may derive from asymmetric and symmetric stretching of carboxyl groups usually identified as diagnostic of gum (see the next paragraph for more details)[47]. These contributions are less intense for samples 1, 34 and 64 (Fig. 2o), allowing the peak centred at about 1,630 cm−1 to arise. All the aforementioned spectral ranges are indicated by the grey shaded areas in Fig. 2o. The collected data led to postulations that the organic fraction is a mixture of two main components: tree or plant gum and beeswax. In particular, the broad peaks in the 1,650–1,550 and 1,450–1,350 cm−1 spectral regions can be associated with carboxylate fractions from plant or tree gum, a natural biopolymer composed mostly of diverse polysaccharides and, to a much lesser extent, glycoproteins[45,48]. This hypothesis was proven by the spectral comparison of samples 75, 106 and 100a with the reference spectrum of tree gum (Fig. 2o) and several other spectra found in the IR databases (see, for example, spectra IDs ICB00011, ICB00012, ICB00013 and ICB00038 in the IRUG database). Pure and fresh gum spectra are characterized by

narrower bands in the aforementioned spectral regions. Nevertheless, it is well known that the peak position of both the asymmetric and symmetric modes of carboxyl groups are strongly dependent on the coordinated cations[44]; therefore, band broadening in our samples reflects the complex mineralcomposition of the soil (see the SEM/EDX analysis and Supplementary Fig. 4 for more details). Reference gum spectra show broad unresolved absorption peaks in the range 3,000–2,800 cm−1, which differ from the signals obtained by measuring our samples that exhibited intense and sharp methyl and methylene stretching modes. This result led to the deduction of the possible addition of a further organic compound to the adhesive, such as beeswax. This hypothesis can be tested by comparison of the collected spectra of samples 1, 34 and 64 with beeswax reference spectra (Fig. 2o). In the literature, the spectra of beeswax (see also IDs IWX00075, IWX00090, IWX00096 and IWX00099 in the IRUG database) are characterized by well-defined and intense methyl and methylene bands, as well as by distinctive carbonyl bands centred at about ~1,740 and ~1,715 cm−1, which were also present in our samples. Among the collected spectra, a variability of the relative intensity of the methylene/methyl/carbonyl bands can be observed, mainly characteristic of beeswax (Fig. 2o), with respect to the broad bands extending from about 1,650–1,550 cm−1 and 1,450–1,350 cm−1, which are characteristic of tree/plant gum (Fig.2o). This finding can be explained by the different percentages of the two organic fractions used to prepare the adhesive mixture, with further consideration of the different degrees of degradation and aging originating from long-term interaction of the organic material constituting the adhesives with the burial soil[46].
The diverse extent of degradation of the samples could have been influenced by differences in soil composition, pH, humidity or water percolation of the stratigraphic units where the ten backed pieces were buried for thousands of years. Identification of the gum fraction would have been easier with access to the ~1,200–900 cm−1 spectral region, where C–O–C and C–OH stretching modes diagnostic of polysaccharides are located46. In this spectral region, very intense and structured bands can be seen for all 10 measured backed pieces. This feature, characterized by a main peak at 1,030 cm−1, a shoulder at 1,080 cm−1 and two distinctive peaks at 800 and 780 cm−1, can be attributed to Si–O stretching modes of silicates, which are the main components of clays. Specifically, the sharp peaks at 3,694 and 3,622 cm−1 are distinctive vibrational features of well-crystallized water molecules among the layers of kaolinite[47].
The red colour of the residues on the backed pieces led us to hypothesize the presence of iron compounds. To verify this hypothesis, SEM/EDX analyses were performed for a soil sample from layer DII and samples 106 (from spit E-D) and 1 (from layer EII-I) after FTIR analysis (Supplementary Fig. 4b,e,h).
EDX measurements of the soil and sample 106 confirmed the presence of silicon, aluminium, magnesium, sodium, calcium, iron and phosphorus, which are all characteristic of silicates. The iron-to-silicon ratio increased from 0.37 ± 0.01 to 4.52 ± 2.01 from the soil to sample 106, reaching a value of 7.64 ± 0.45 in sample 1 (the standard deviation was calculated as the average of three measurements per sample). The positive trend of the iron-to-silicon ratio from the soil to sample 1 is consistent with a colour transition from light brown to intense red (Supplementary Fig. 4a,d,g), revealing that the iron content of the samples is much higher than the one of the burial soil and that it contributes to red pigmentation of the residues on samples 1 and 106, which can be identified as ochre.
To further verify that ochre (also known as red earth) is the source of the red colour, some red soil deposits collected from Grotta del Cavallo were analysed by FTIR spectroscopy in the FIR-MIR region. These deposits belong to the same stratigraphic units (layers E and D) as the analysed

backed pieces (see Supplementary Fig. 1). In Supplementary Fig. 5, we report the FIR-MIR spectra of two of the analysed red deposits. It is possible to identify peaks centred at about 535 and 433 cm−1, as well as a broad band around 325 cm−1, that are distinctive of iron oxides. The collected spectra can be correlated with the IRUG ochre spectrum IMP00365 (red earth made by kaolinite and hematite). Supplementary Fig. 5 also reports the FIR-MIR spectrum of the soil sample from layer DII, also analysed by SEM/EDX (Supplementary Fig. 4). This sample does not show the spectral features characteristic of ochre, accordingly with the minimal iron content revealed by SEM/EDX analysis; instead, it is mainly characterized by a mixture of silicates and phosphates. As a matter of fact, the silicate peaks described above can also be recognized in the FTIR spectrum of the soil, and distinctive features of phosphates can be also identified: two sharp peaks at ~964 and ~870 cm−1, a double peak at ~605 and ~564 cm−1 and a moderate absorption band in the 1,550–1,300 cm−1 spectral range49. The aforementioned phosphate infrared features are still evident in the spectrum of the red deposit from layer D, whereas they are barely detectable for the red deposit from layer E II-I. This result implies that the red deposit from layer D is partially contaminated by the burial soil, whilethe one from layer E II-I can be considered as a purer ochre. None of the spectra reported in Supplementary Fig. 5 show absorbance peaks in the region 3,000–2,800 cm−1, which are characteristic of aliphatic chains of organic compounds. This result suggests that, in both the soil and red deposits, the organic matter content is below the detection limit of the technique, thereby excluding the possibility that the organic traces on backed pieces are contamination from the burial environment. Taken together, these results led us to conclude that the residue stuck on the backed pieces is a mixture of plant/tree gum and beeswax intentionally mixed with ochre and applied as an adhesive.

Morphometric analysis. As the Uluzzian backed pieces are extremely small (Supplementary Figs. 6a and 7b), they are not suitable to haft onto the tips of thick wooden spears from Schöningen in Germany dated ~300 ka[50–52], which were probably used as throwing spears[53,54] (Supplementary Fig. 7a). It has been ethnographically shown that thrusting spears and hand-delivered spears are heavier than projectile spears launched with a spearthrower or bow[55,56]. Therefore, the Uluzzian backed pieces do not function well as throwing or thrusting spear tips, which require a massive shaft. If the Uluzzian backed pieces were inserted into the lateral sides of a shaft as in Magdalenian composite projectiles[57], the smallness of the stone artefacts would not necessarily relate to the diameter of the shaft. However, as the use-wear analysis suggested that a considerable number of Uluzzian pieces were attached to the tip of a shaft as a hunting armature, the small dimensions must reflect a thin shaft that is useful only for mechanically delivered spears, such as darts projected by a spearthrower or arrows shot using a bow. A morphometric analysis using TCSA and TCSP values was therefore undertaken to evaluate the potential projectile capability of stone tips[20,56,58,59].

TCSA and TCSP values of Uluzzian backed pieces from Grotta del Cavallo were compared with those of ethnographic North American dart tips and arrowheads[12,13]. Because some Uluzzian backed pieces were used for cutting and scraping, the TCSA and TCSP analyses were undertaken only for the backed pieces showing DIFs (Supplementary Fig. 6b,c). The TCSA and TCSP values were calculated using the equations presented by Sisk and Shea [59].

Acknowledgements We thank Soprintendenza Archeologia, Belle Arti e Paesaggio per le Province di Brindisi, Lecce e Taranto, and especially Drs. Maria Piccarreta and Serena Strafella for kindly supporting our research at Grotta del Cavallo. Special thanks are due to Professors Arturo Palma di Cesnola and Paolo Gambassini for giving us the opportunity to revisit the Uluzzian materials from

their excavations. We are grateful to Professor Lucia Sarti for providing the base planimetry of Grotta del Cavallo. We also acknowledge Elettra Sincrotrone Trieste for provision of synchrotron radiation facilities (proposal No. 20180262) and Weizmann Institute of Science for providing the Kimmel Center for Archaeological Science Infrared Standards Library. Finally, we thank Professor Ilaria Corsi for providing contacts between the University of Siena and Elettra Sincrotrone Trieste. This research was supported by a grant from the European Research Council (ERC-724046, SUCCESS; http://www.erc-success.eu/). K.S. was supported by MEXT/JSPS KAKENHI grant numbers JP17H06381 in #4903 and 15H05384.

Author Contributions

A.M. and K.S. conceived and organized the project; S.B. obtained funding and directed the project; K.S. undertook the use-wear analysis with S.A as well as the morphometric analysis; C.S., G.B., and L.V. performed the residue analysis; D.A. conducted the experiment for producing Uluzzian backed pieces; I.F., M.G., and A.T. provided data about the exploitation of feathers; F.B., J.C., and P.B. presented the results of the zooarchaeological analysis; K.S., C.S., V.S., S.R., and I.F made figures and illustrations; D.A., F.B., A.R., and A.M. provided permits for the analysis of the archaeological samples and expertise on site sequences and materials; and K.S., C.S., A.R., A.M., and S.B. wrote the manuscript with contributions from all co-authors.

Competing interests The authors declare no competing interests.

Correspondence and requests for materials and data should be addressed to K.S.

Captions

Fig. 1 | Locations of the Uluzzian findings in Italy and on the Balkan Peninsula. 1, Klissoura Cave; 2, Kephalari Cave; 3, Crvena Stijena; 4, Grotta del Cavallo; 5, Grotta di Serra Cicora A; 6, Grotta Mario Bernardini; 7, Grotta di Uluzzo; 8, Grotta di Uluzzo C/Cosma; 9, Grotta delle Veneri; 10, Grotta di Castelcivita; 11, Grotta della Cala; 12, Colle Rotondo; 13, Grotta La Fabbrica; 14, Riparo del Broion; 15, Grotta di Fumane. Sea level is 74 m below the presentdaycoastline (data from ref. 60). The digital elevation model is the European digital elevation model from the GMES RDA project (https://www.eea.europa.eu/data-and-maps/data/eu-dem#tab-originaldata/eudem_hlsd_3035_europe). The bathymetric model is from the European Marine Observation and Data Network. The map was generated using ArcGIS version 10.5.

Fig. 2 | Backed pieces from Grotta del Cavallo showing DIFs and MLITs, and sampling of residues on backed pieces by FTIR spectroscopy and its results. **a**, A simple DIF type a2. **b**–**f**, Multiple DIF type a2m. **a**(i), **c**(ii) and **d**(i) are burin-like fractures; **b**(i), **c**(i) and **c**(iii) are flute-like fractures; **b**(ii) is a step-terminating transverse fracture and a spin-off; **e**(i) and **d**(ii) are spin-offs; **e**(ii) is a step-terminating transverse fracture; **f**(ii) is flute- and burin-like fractures; **f**(iii) is a feather-terminating transverse fracture. **a**(ii), **f**(i) and the black lines in **a** and **f** are MLITs. **b**, **c** and **e** are from layer EII-I; **a** and **d** are from layer E-D; and **f** is from layer D. **g**,**k**, Optical images at two different angles of sample 1, layer EII-I (scale bar, 5 mm) and sample 106, spit E-D (scale bar, 5 mm). Sampled areas

are highlighted by a black box and magnified in **h** and **i** for sample 1 (scale bars, 1 mm and 0.5 mm) and in **l** and **m** for sample 106 (scale bars, 2 mm and 1 mm). **j**,**n**, Optical images of the scraped residues sitting on the culet of the opened diamond compression cell. **o**, Representative FTIR spectra of the sampled residues from samples 1, 34, 64, 75, 106 and 100a. Two selected reference spectra of beeswax and peach tree gum are also plotted using the database from the Kimmel Center for Archaeological Science Infrared Standards Library (https://www.weizmann.ac.il/kimmel-arch/infrared-spectra-library). The grey shaded areas indicate the main absorption bands, characteristic of the organic fraction. Among them, those relating to beeswax are marked with dagger symbols, and those relating to plant/tree gum are marked with section symbols. For more details on the band positions and assignments, refer to the Methods.

References

1. Moroni, A. et al. *J. Anthr. Sci.* **96**, 125–160 (2018).
2. Zanchetta, G., Giaccio, B., Bini, M. & Sarti, L. *Quat. Sci. Rev.* **182**, 65–77 (2018).
3. Giaccio, B., Hajdas, I., Isaia, R., Deino, A. & Nomade, S. *Sci. Rep.* **7**, 45940 (2017).
4. d'Errico, F., Borgia, V. & Ronchitelli, A. *Quat. Int.* **259**, 59–71 (2012).
5. Moroni, A., Boscato, P. & Ronchitelli, A. *Quat. Int.* **316**, 27–44 (2013).
6. Palma di Cesnola, A. *Riv. Sci. Preist.* **21**, 3–59 (1966).
7. Fischer, A., Hansen, P. V. & Rasmussen, P. *J. Dan. Archaeol.* **3**, 19–46 (1984).
8. Sano, K. & Oba, M. *J. Archaeol. Sci.* **63**, 13–23 (2015).
9. Bradtmöller, M., Sarmiento, A., Perales, U. & Zuluaga, M. C. *J. Archaeol. Sci. Rep.* **7**, 1–13 (2016).
10. Yaroshevich, A., Kaufman, D., Nuzhnyy, D., Bar-Yosef, O. & Weinstein-Evron, M. *J. Archaeol. Sci.* **37**, 368–388 (2010).
11. Goldstein, S. T. & Shaffer, C. M. *Archaeol. Anthr. Sci.* **9**, 1767–1788 (2017).
12. Thomas, D. H. *Am. Antiq.* **43**, 461–472 (1978).
13. Shott, M. J. *Am. Antiq.* **62**, 86–101 (1997).
14. Wadley, L. *J. Hum. Evol.* **49**, 587–601 (2005).
15. Cattelain, P. *Bull. Soc. Préhist. Fr.* **86**, 213–216 (1989).
16. Rust, A. *Die alt- und Mittelsteinzeitlichen Funde von Stellmoor* (Karl Wachholtz, 1943).
17. Stodiek, U. *Zur Technologie der Jungpaläolithischen Speerschleuder: Eine Studie auf der Basis Archäologischer, Ethnologischer und Experimenteller Erkenntnis* (Archaeologica Venatoria, Institut für Ur- und Frühgeschichte der Universität Tübingen, 1993).
18. Thieme, H. & Veil, S. *Ldkr. Verden Kunde* **36**, 11–58 (1985).
19. Villa, P., Boscato, P., Ranaldo, F. & Ronchitelli, A. *J. Archaeol. Sci.* **36**, 850–859 (2009).
20. Shea, J. J. *J. Archaeol. Sci.* **33**, 823–846 (2006).
21. Metz, L. in *Le Troisième Homme Préhistoire de l'Altaï* 156–160 (Musée National de la Préhistoire, 2017).
22. Slimak, L. *Quat. Sci. Rev.* **217**, 330–339 (2019).
23. Villa, P. & Soriano, S. *J. Anthropol. Res.* **66**, 5–38 (2010).
24. Wadley, L. & Mohapi, M. *J. Archaeol. Sci.* **35**, 2594–2605 (2008).
25. Zilhão, J., Banks, W. E., d'Errico, F. & Gioia, P. *PLoS ONE* **10**, e0131181 (2015).
26. Benazzi, S. et al. *Nature* **479**, 525–528 (2011).

27. Heptner, V. G., Nasimovich, A. A. & Bannikov, A. G. *Mammals of the Soviet Union* Vol. 1 (Smithsonian Institution Libraries, National Science Foundation, 1988).
28. Lew-Levy, S., Reckin, R., Lavi, N., Cristóbal-Azkarate, J. & Ellis-Davies, K. *Hum. Nat.* **28**, 367–394 (2017).
29. Milks, A., Parker, D. & Pope, M. *Sci. Rep.* **9**, 820 (2019).
30. Tringham, R., Cooper, G., Odell, G., Voytek, B. & Whitman, A. *J. Field Archaeol.* **1**, 171–196 (1974).
31. Odell, G. H. & Odell-Vereecken, F. *J. Field Archaeol.* **7**, 87–120 (1980).
32. Odell, G. H. *J. Field Archaeol.* **8**, 197–209 (1981).
33. Akoshima, K. in *The Human Uses of Flint and Chert: Proc. Fourth International Flint Symposium Held at Brighton Polytechnic 10-1 April 1983* (eds Sieveking, G. D. & Newcomer, M. H.) 71–79 (Cambridge Univ. Press, 1987).
34. Keeley, L. H. *Experimental Determination of Stone Tool Uses: A Microwear Analysis* (Univ. Chicago Press, 1980).
35. Vaughan, P. C. *Use-Wear Analysis of Flaked Stone Tools* (Univ. Arizona Press, 1985).
36. Van Gijn, A. L. *The Wear and Tear of Flint: Principles of Functional Analysis Applied to Dutch Neolithic Assemblages* (Univ. Leiden, 1990).
37. Sano, K. *Functional Variability in the Late Upper Palaeolithic of North-Western Europe* (Rudolf Habelt, 2012).
38. Lombard, M. *J. Archaeol. Sci.* **35**, 26–41 (2008).
39. Pargeter, J. *J. Archaeol. Sci.* **40**, 4056–4065 (2014).
40. Sano, K. *Quartär* **56**, 67–86 (2009).
41. Pargeter, J. *J. Archaeol. Sci.* **38**, 2882–2888 (2011).
42. Moss, E. H. & Newcomer, M. H. *Stud. Praehist. Belg.* **2**, 289–312 (1982).
43. Geneste, J. M. & Plisson, H. in *Before Lascaux: The Complex Record of the Early Upper Paleolithic* (eds. Knecht, H. et al.) 117–135 (CRC, 1993).
44. Lupi, S. et al. *J. Opt. Soc. Am. B* **24**, 959–964 (2007).
45. Petrea, P., Amarioarei, G., Apostolescu, N., Puitel, A. C. & Ciovica, S.*Cell. Chem. Technol.* **47**, 369–375 (2013).
46. Socrates, G. in *Infrared and Raman Characteristic Group Frequencies Tables and Charts* (ed. Socrates, G.) 283–340 (Wiley, 2001).
47. van der Marel, H. W. & Krohmer, P. *Contr. Mineral. Petrol.* **22**, 73–82 (1969).
48. Espinosa-Andrews, H., Sandoval-Castilla, O., Vazquez-Torres, H., Vernon-Carter, E. J. & Lobato-Calleros, C. *Carbohydr. Polym.* **79**, 541–546 (2010).
49. Fleet, M. E. *Biomaterials* **30**, 1473–1481 (2009).
50. Sierralta, M., Frechen, M. & Urban, B. in *Die Chronologische Einordnung der Paläolithischen Fundstellen von Shöningen: Forschungen zur Urgeschichte aus dem Tagebau von Schöningen Band 1* (ed. Behre, K.-E.) 143–154 (Römisch-Germanischen Zentralmuseums, 2012).
51. Urban, B. & Sierralta, M. in *Die Chronologische Einordnung der Paläolithischen Fundstellen von Shöningen: Forschungen zur Urgeschichte aus dem Tagebau von Schöningen Band 1* (ed. Behre, K.-E.) 77–96 (Römisch-Germanischen Zentralmuseums, 2012).
52. Richter, D. & Krbetschek, M. *J. Hum. Evol.* **89**, 46–56 (2015).
53. Thieme, H. *Nature* **385**, 807–810 (1997).

54. Thieme, H. in *The Hominid Individual in Context: Archaeological Investigations of Lower and Middle Palaeolithic Landscapes, Locales and Artefacts* (eds Gamble, C. & Porr, M.) 115–132 (Routledge, 2005).
55. Cattelain, P. in *Projectile Technology* (ed. Knecht, H.) 213–240 (Plenum, 1997).
56. Hughes, S. S. *J. Archaeol. Method Theory* **5**, 345–408 (1998).
57. Pétillon, J.-M. et al. *J. Archaeol. Sci.* **38**, 1266–1283 (2011).
58. Shea, J. J. & Sisk, M. L. *Paleoanthropology* **2010**, 100–122 (2010).
59. Sisk, M. L. & Shea, J. J. *Int. J. Evolut. Biol.* **2011**, 1–8 (2011).
60. Waelbroeck, C. et al. *Quat. Sci. Rev.* **21**, 295–305 (2002).

Fig. 1

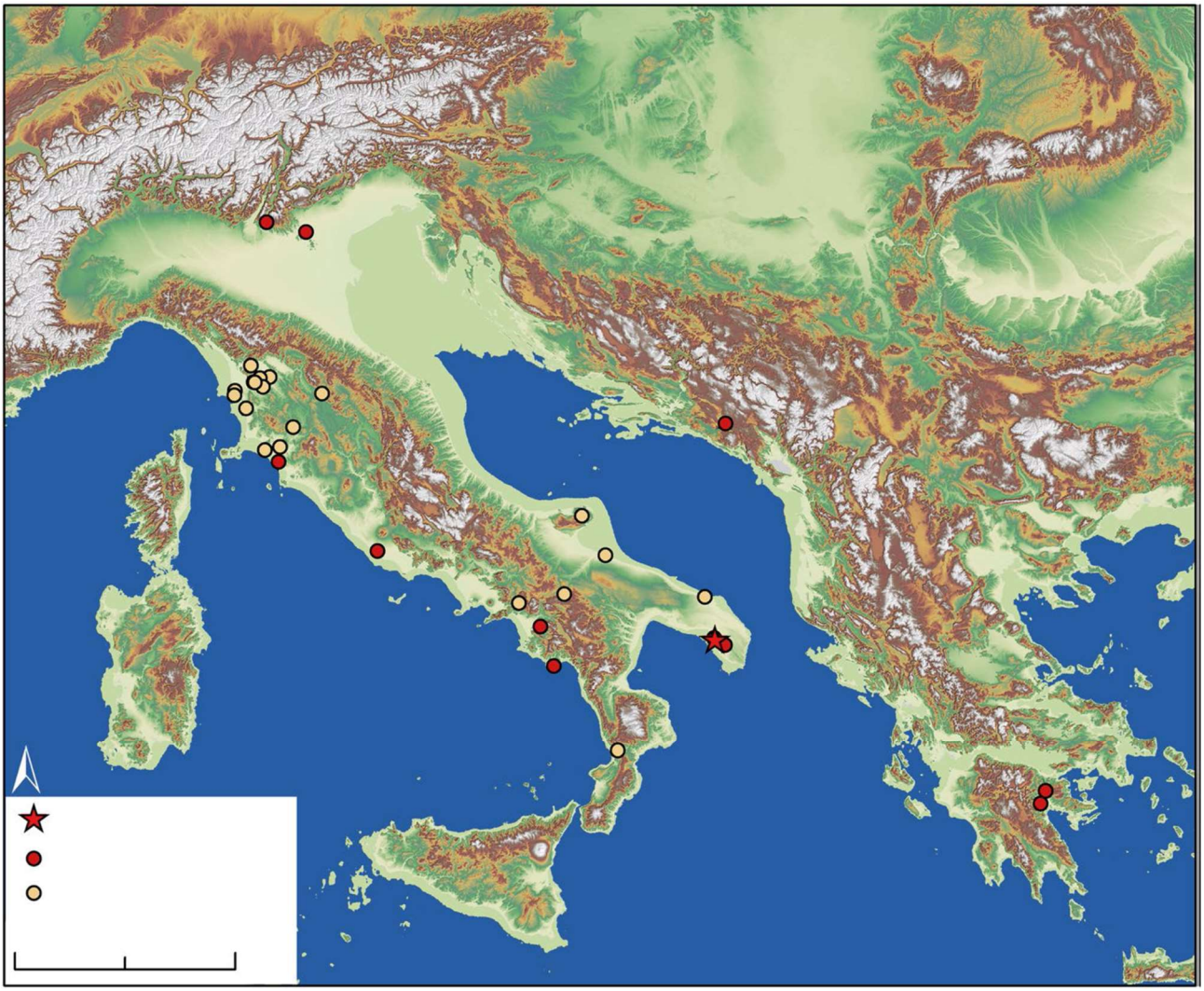

Fig. 2

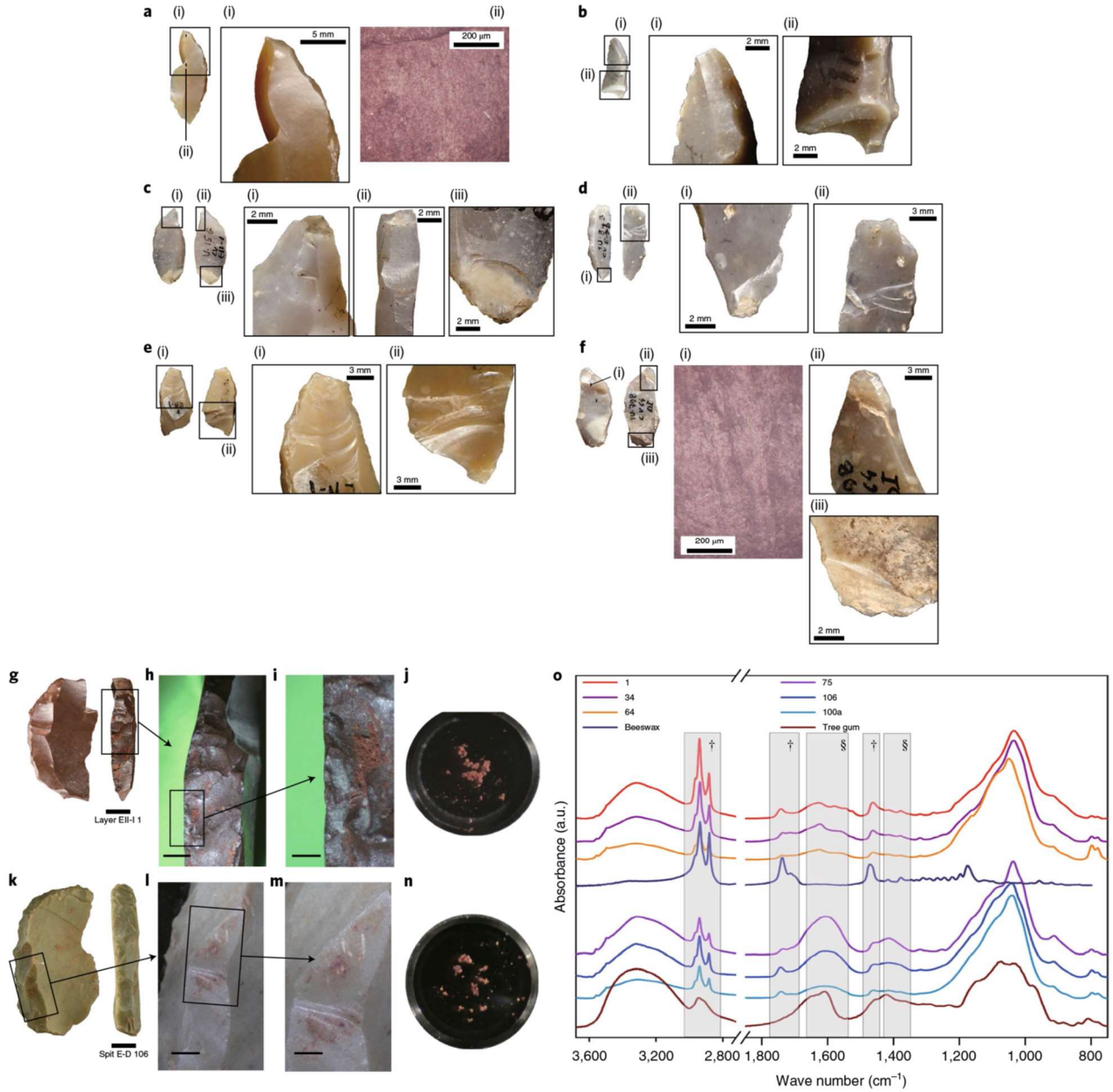
a
b
c
d
e
f
g
h
i
j
k
l
m
n
o
5 mm
200 µm
2 mm
3 mm
Layer EII-I 1
Spit E-D 106
1
34
64
Beeswax
75
106
100a
Tree gum
Absorbance (a.u.)
3,600
3,200
2,800
1,800
1,600
1,400
1,200
1,000
800
Wave number (cm−1)